Ab Initio Topological Analysis of the Electronic Density in Proponium Cations

Nora Okulik,[†] Nélida Peruchena,[‡] Pierre M. Esteves,[§] Claudio Mota,[§] and Alicia H. Jubert*[,‖]

Facultad de Agroindustrias, UNNE, Cte. Fernández 755, (3700) Pcia. R. Sáenz Peña, Chaco, Argentina, Departamento de Química, Facultad de Ciencias Exactas y Naturales y Agrimensura, UNNE, Av. Libertador 5300, (3400) Corrientes, Argentina, Instituto de Química, Departamento de Química Orgânica, Universidade Federal de Río de Janeiro, 21949-900, Río de Janeiro, Brazil, and CEQUINOR, Centro de Química Inorgánica (CONICET, UNLP), Departamento de Química, Facultad de Ciencias Exactas, UNLP, C. C. 962, 1900 La Plata, Argentina

Studies performed on proponium cations at the ab initio level show that six different stable structures can be characterized: four proponium cations and two van der Waals complexes. Among the proponium cations, the most stable structure corresponds to the C-proponium ion. Between the van der Waals complexes, the most stable one correponds to the structure that results from the interaction between the isopropyl ion and the hydrogen molecule. The topology of the electronic density charge of the different structures is studied, at ab initio level, using the theory of atoms in molecules (AIM) developed by Bader.

Introduction

The protonation of alkanes in superacid systems was independently studied by Olah[1,2] and Hogeveen.[3] Superacids are so strong as acids that they can protonate extremely weak bases, such as alkanes. These media presents very low nucleophilicity not attacking the formed carbocations, which remain stable in these media. The protonation of alkanes in liquid superacids provided evidence for the formation of pentacoordinated carbonium ions. These species contain three center–two electron bonds generated upon the insertion of a proton in the C–H and C–C bonds.

The concept of σ basicity introduced by Olah[4,5] has been extended to solid acids, especially zeolites.[6–9] The connection between hydrocarbon reactions in superacids media and on zeolites naturally carries on the interest to inquire on the mechanism of electrophilic activation of alkanes in both media and are of great importance in petrochemical processes.

Because of the shortage of direct experimental observation of carbonium ions, their structure and energy have been mostly studied by theoretical methods. The use of ab initio calculations, particularly those including electron correlation effects, has proven to provide excellent prediction for the energy and geometry for the methonium and ethonium cations.[10–24] However, ions with a larger number of carbon atoms have not been studied in depth.

The molecular charge distribution (ρ) topology yields a single unified theory of molecular structure, which defines atoms, bonds, structure, and the mechanism of structural changes.[25,26] The same theory defines all average properties of an atom in a molecule.[27]

One may, unambiguously, assign a chemical structure to a molecule by determining the number and kind of critical points (c.p.) in its electronic charge distribution. The critical points

are located where $\nabla\rho = 0$. The same information enables one to determine whether or not the structure is topologically stable with respect to the making and/or breaking chemical bonds. If it is unstable, one may predict the possible ensuing structural changes. The determination of the kind and number of critical points, and thereby, the structure of a molecule is, computationally, a straightforward procedure, being comparable in its simplicity of implementation and computer time with the requirements of a Mulliken population analysis.[28] It is shown that chemical information about a molecular system is usefully summarized and economically extracted from its charge distribution in terms of the properties of ρ at its critical points.

In this work the topology of the electronic density charge is studied for $C_3H_9{}^+$ species shown in Figure 1, at ab initio level, using the Theory of Atoms in Molecules (AIM) developed by Bader.[26,27] The electronic delocalization that operates through the σ bonds in saturated molecules and specifically in protonated alkanes, can be studied by means of the analysis of the charge density and the bond critical points.

The ellipticity provides a sensitive measure of the susceptibility of a system to undergo a structural change. Therefore, predictions of structural changes in the geometry of the proponium cations will be presented on the basis of the properties of bond ellipticity, and the curvature of the bond path, all of them defined in terms of a system's charge distribution.[29,30] In a previous work[31] the topology of the electronic density charge of the isobutonium cations was studied, at the ab initio level, using the AIM theory[26,27] Five different structures were studied: three isobutonium cations and two van der Waals complexes. Among the isobutonium cations, the most stable structure corresponds to the C-isobutonium ion. A shared and a van der Waals interaction was characterized due to their topological properties. The H-isobutonium cations were significantly higher in energy. Because of the characterization of an unstable critical point and the larger ellipticity found for the C_2–H* and H*–H* bonds, it was possible to understand why these species undergo a structural change, explaining the easy transformation between structures. The two i-$C_4H_{11}{}^+$ structures

---

Electronic Density in Proponium Cations

J. Phys. Chem. A, Vol. 104, No. 32, 2000 **7587**
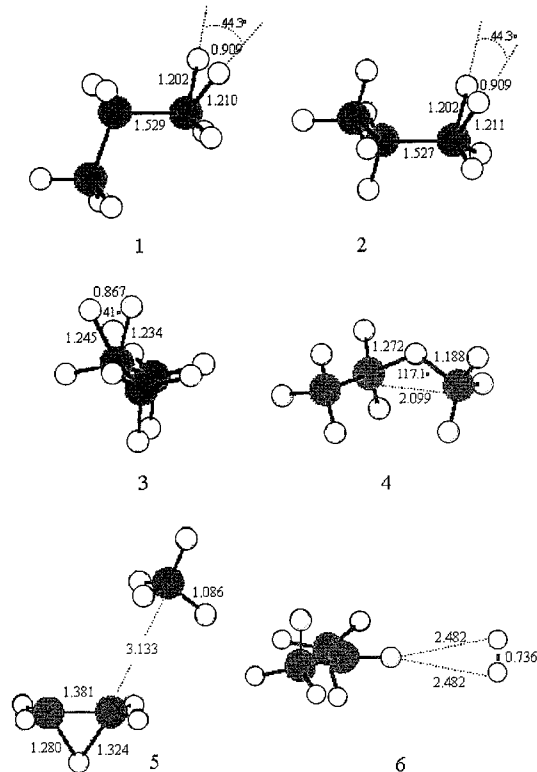
Figure 1. Structures **1**−**6**. MP4(SDTQ)/6-311++G**/MP2(full)/6-31G** geometries of $C_3H_9^+$ isomers.

most energetically favored correspond to the van der Waals complexes: one involving CH_4 and the isopropyl cation and the other, the lowest in energy, between H_2 and the *tert*-butyl cation. The topological study of the charge density reveals that in the complex a delocalization of the electronic density takes place on the three carbons atoms of the methyl groups. In this way, the last van der Waals complex is stabilized and happens to be the most energetically favored structure.

Esteves et al.[32] had calculated the potential energy surface of the $C_3H_9^+$ cation, that results form the protonation of propane, at the MP4(SDTQ)/6-311++G**//MP2(full)/6-31G** level of calculation. They were able to characterize six structures as minima on the potential energy surface. In addition to the four proponium cations, hypothetically formed by protonation in the primary C−H bond (**1** and **2**, Figure 1), secondary C−H bond (**3**, Figure 1) and C−C bond (**4**, Figure 1) of propane, two van der Waals complexes were also characterized as minima in the potential energy surface. Structure **5** (Figure 1) represents the complex formed between the ethyl cation and methane and structure **6** (Figure 1) the complex formed between the isopropyl cation and hydrogen. At MP4/6-311++G**//MP2/6-31G** level, the C-proponium cation (**4**) was the lowest energy species with the van der Waals complex formed between the isopropyl cation and hydrogen (**6**) lying only 0.3 kcal/mol above. The H-proponium ions were significantly higher in energy. The 2-H-proponium was about 7 kcal/mol and the 1-H-proponium about 10 kcal/mol higher than structure **4**. The C-proponium cation (stucture **3**) was lower in energy than the H-proponium structures **1** and **2** that have nearly the same energy.

Computational Details

Calculations, at Hartree−Fock single reference second and fourth order Møller−Plesset perturbation theory (MP2 and MP4), were performed for the proponium cations and the van

der Waals complexes. The fully optimized molecular geometries were characterized as minima in the potential energy surface by the absence of imaginary vibrational frequencies. Calculations were carried out with the Gaussian 94[33] and GAMESS US[34] packages of molecular orbital programs using the 6-31G ** and 6-311++G** basis sets.

The topological properties of the charge density distribution were carried out using 6-311++G** basis sets at HF and MP2 (structure 6) level of calculations. The local topological properties of the electronic charge density in the bonds critical points were obtained with the package of programs AIMPAC.[35] The c.p. of the charge distribution, (points of the distribution where $\nabla\rho = 0$) are classified by their rank (w) and the signature (σ), the algebraic sum of the signs of the curvatures of ρ, as (w,σ). Four types of c.p. can be characterized. At a $(3,-3)$ critical point, all three curvatures (obtained from the Hessian matrix of ρ) are negative, at a $(3,+3)$ critical point all curvatures are positive and ρ is a local minimum at r_c a $(3,-1)$ critical point possesses two negatives and one positive curvature, and at a $(3,+1)$, or ring critical point, two curvatures are positive and one is negative. The critical points presenting three non null eigenvalues, two negative (λ_1 and λ_2) and one positive, (λ_3), correspond to bond critical points $(3,-1)$ and they will be analyzed in this study.

In this paper, bond ellipticity (ϵ) is defined in terms of the charge density value and its principal curvature at a bond critical point ($\epsilon = \lambda_1/\lambda_2 - 1$). The ellipticity measures the deviation of the charge distribution of a bond path from axial symmetry. In terms of the orbital model of electronic structure, the ellipticity provides a quantitative measure of the π character of a bond on the direction of its major axis.[36]

The Laplacian $\nabla^2\rho(r)$ is associated with the charge density. It is the sum of the curvatures in the electron density along any orthogonal coordinate axes at the point (r). The sign of $\nabla^2\rho(r)$ indicates whether the charge density is locally depleted [$\nabla^2\rho(r) > 0$] or locally concentrated [$\nabla^2\rho(r) < 0$].

A molecular graph is the network of bond paths linking pairs of neigbouring nuclei. The molecular graph for a molecule at an equilibrium geometry is identified with the corresponding network of chemical bonds.

The Laplacian of the charge density defines the chemically important valence-shell charge concentration, the shell of charge concentration which, upon chemical combination, is distorted to yield maxima corresponding in number and relative position to the electron pairs[37] anticipated by the Lewis and related models, such as the VSEPR model of molecular geometry.[38] The description of these changes requires a study of the topology of the Laplacian distribution.

Extrema in the Laplacian of ρ are classifed by rank and signature in the same way as are critical points in the charge density. The critical points in the Laplacian occur where $\nabla(\nabla^2\rho) = 0$ and the eigenvalues of the Hessian of $\nabla^2\rho$ are the principal curvatures of $\nabla^2\rho$ at the critical point. The topological discussions will always refer to the negative of the Laplacian, the quantity $-\nabla^2\rho$. Since charge is concentrated where $\nabla^2\rho < 0$, a local maximum in $-\nabla^2\rho$ is synonymous with a maximum in the concentration of electronic charge. Thus, a local maximum in $-\nabla^2\rho$, a $(3,-3)$ critical point with $\nabla^2\rho < 0$, will denote a local concentration in electronic charge and a local minimum in $-\nabla^2\rho$, a $(3,+3)$ critical point, and, with $\nabla^2\rho > 0$, will denote a local depletion in electronic charge.

The outer quantum shell of an atom is divided into an inner region over which $\nabla^2\rho < 0$ and an outer region over which $\nabla^2\rho > 0$. The portion of the shell over which $\nabla^2\rho < 0$, is called

TABLE 1: Local Topological Properties in the Bond Critical Points (3,−1) of the Structures 1, 2, and 3[a]

bond	R	$\rho(r_c)$	$\nabla^2\rho(r_c)$	λ_1	λ_2	λ_3	$|\lambda_1|/\lambda_3$	e
C_1−C_2	1,529	0,2414	−0,6581	−0,4307	−0,4260	0,1986	2,1687	0,0112
	(1,527)	(0,2431)	(−0,6645)	(−0,4379)	(−0,4263)	(0,1997)	(2,1928)	(0,0274)
	[1,524]	[0,2487]	[−0,6840]	[−0,4592]	[−0,4486]	[0,2237]	[2,0527]	[0,0236]
C_2−C_3	1,525	0,2516	−0,6781	−0,4728	−0,4703	0,2650	1,7841	0,0054
	(1,522)	(0,2546)	(−0,6913)	(−0,4823)	(−0,4783)	(0,2692)	(1,7916)	(0,0841)
	[1,524]	[0,2486]	[−0,6838]	[−0,4591]	[−0,4485]	[0,2237]	[2,0523]	[0,0237]
C_1−H	1,101	0,2746	−0,9765	−0,7239	−0,7135	0,4610	1,5703	0,0144
	(1,102)	(0,2747)	(−0,9763)	(−0,7246)	(−0,7119)	(0,4602)	(1,5745)	(0,0179)
	[1,086]	[0,2864]	[−1,0445]	[−0,7528]	[0,7405]	[0,4488]	[1,6774]	[0,0166]
C_2−H	1,088	0,2891	−1,0621	−0,7571	−0,7422	0,4371	1,7321	0,0200
	(1,087)	(0,2899)	(−1,0660)	(−0,7619)	(−0,7456)	(0,4415)	(1,7257)	(0,0218)
	[1,100]	[0,2817]	[−1,0206]	[−0,7420]	[−0,7398]	[0,4612]	[1,6088]	[0,0029]
C_3−H	1,086	0,2863	−1,0422	−0,7454	−0,7362	0,4393	1,6968	0,0125
	(1,085)	(0,2865)	(−1,0438)	(−0,7479)	(−0,7394)	(0,4435)	(1,6863)	(0,0114)
	[1,086]	[0,2864]	[−1,0446]	[−0,7528]	[−0,7405]	[0,4488]	[1,6774]	[0,0166]
C_n−H* (°)	1,210	0,2125	−0,4089	−0,3572	−0,1267	0,0750	4,7626	1,8179
	(1,211)	(0,2123)	(−0,4081)	(−0,3574)	(−0,1276)	(0,0769)	(4,6476)	(1,8015)
	[1,245]	[0,1946]	[−0,2276]	[−0,2544]	[−0,1145]	[0,1413]	[1,8004]	[1,2227]
H*−H*	0,909	0,2198	−0,5849	−0,5542	−0,2109	0,1802	3,0755	1,6274
	(0,909)	(0,2197)	(−0,5852)	(−0,5553)	(−0,2140)	(0,1841)	(3,0163)	(1,5945)
	[0,867]	[0,2267]	[−0,6844]	[−0,6192]	[−0,3542]	[0,2890]	[2,1425]	[0,7482]

[a] Bond distances are included. (°) $n = 1$ for structures 1 and 2 and $n = 2$ for structure 3. Bond distances are expressed in angstroms, and $\rho(r)$ and $\nabla^2\rho(r)$ are expressed in au.

valence-shell charge concentration or VSCC. Within this shell is the sphere over whose surface the valence electronic charge is maximally and uniformly concentrated.

Each point in the surface of the sphere of maximum concentration in the VSCC is a $(1,−1)$ critical point. In general this surface persists when the atom is in chemical combination, but the sphere is distorted and the surface has not an uniform concentration, as the two tangencial curvatures assume either positive or negative values. The topology of the Laplacian of ρ on this surface is equivalent to the description of the hills and valleys of a surface terrain. If a local maximum is formed on the surface, then the two tangential curvatures are negative and the result is a $(3,−3)$ critical point in $−\nabla^2\rho$. If the two tangential curvatures assume positive values, a local minimum is formed on the surface and the result is a $(3,+1)$ critical point in $−\nabla^2\rho$. If the two curvatures assume values of opposite sign, there is a saddle point on the surface and the result is a $(3,−1)$ critical point in $−\nabla^2\rho$. The local maxima that are created within the VSCC provide a one-to-one mapping of the electron pairs of the Lewis model, both bonded and nonbonded. VSCC was used to characterize a 3c−2e bond.

Results and Discussion

Proponium Cations. Table 1 shows the more significant topological local properties at the critical points, c.p. $(3,−1)$ or bond critical points, for structures **1** and **2** (between parenthesis) and **3** (between brackets) corresponding to the H-proponium cations. We have also included the bond distances for comparison purposes.

The topological distribution of the electronic charge density on the H-proponium cation **1**, shows nearly no differences with respect to structure **2**. In the 1-H-proponium cations, the three center bond $C_{(1)}$−H*−H*, on the primary carbon, is energetically less stable than that on the secondary carbon, 2-H-proponium (structure **3**). The electronic density at the c.p. of the C−H* bonds of the three center bond $C_{(1,2)}$−H*−H* are rather different. In fact, the density in the bond c. p. of $C_{(1)}$−H*, the primary H-carbonium ion, is higher than the density in the $C_{(2)}$−H*, a secondary H-carbonium ion. Both c.p. show different topological characteristics, in function of the values of the curvatures, allowing us to characterize both c.p. $C_{(1,2)}$−
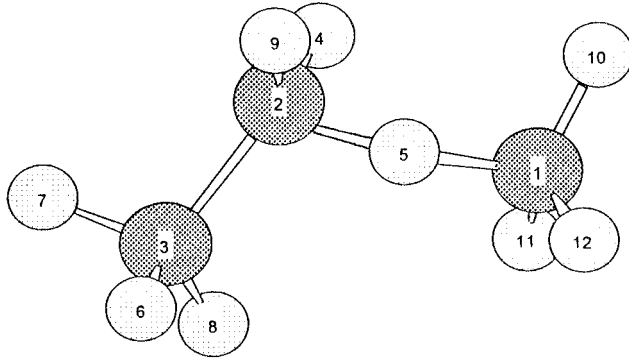
H* as a shared interaction. In these 3c−2e bonds, the Laplacian of the density $(\nabla^2\rho(r_c))$ is negative and $|\lambda_1|/\lambda_3$ is > 1; $(\rho(r_c) = 0.2125$ au, 0.1946 au and $\nabla^2\rho(r_c) = -0.4089, −0.2276$ au for structures **1** and **3**, respectively). If we compare the local properties of the $C_{(1,2)}$−H* bond with the other carbon hydrogen bonds of the methyl group (taken as reference bonds) one can see that both, the density and the Laplacian values, are diminished, indicating a weaker interaction. The ellipticities of these bonds are significantly high. It can be observed in Table 1 that the bond distance $C_{(2)}$−H in structures **1, 2** and **3** are 1.088, 1.087 and 1.100 Å, respectively. The bond c.p. $C_{(2)}$−H, exhibits the characteristics of a shared interaction, where $\rho(r_c)$ takes a value of 0.2891, 0.2899, and 0.2817 au, respectively, for structures **1, 2** and **3**, and $\nabla^2\rho(r_c)$ is negative, $(−1.0621$ au, $−1.0660$ au, -1.0206 au, respectively). In these cases, it is also proven that the relationship, $|\lambda_1|/\lambda_3 > 1$, (1.7321, 1.7257 and 1.6088) as it is generally found for shared interactions. It is interesting to note that the ellipticity, ϵ, of the $C_{(2)}$−H bond in structures **1** and **2** are higher than in the other C−H bonds ($\epsilon = 0.0200, 0.0218$), while that one corresponding to the structure **3** has the lowest value (0.0029). Since the ellipticity arises from the relationship among the negative curvatures along perpendicular axes to the bond path ($\epsilon = \lambda_1/\lambda_2 − 1$), its increase is a measure of how far the density distribution is distorted from the axial symmetry in the bond ($\lambda_1 \neq \lambda_2$).

To confirm de Bader's shared interaction character of the 3c−2e bond we compared its topological properties with that from N−B bond in the $F_3B:NH_3$ molecule. We report values for the density of the potential and kinetic energies ($V(r)$ and $G(r)$) evaluated at the bond critical points for N−H (Bader's shared interaction) and N−B (intermediate interaction) and C_1−H*, C_2−H* bonds from structure **4**: $V(r)$: $−0.5733$, $−0.013621, −0.2851, −0.2055$, respectively and $G(r) = 0.0453$, 0.1512, 0.0894, 0.0812, respectively. The values of $V(r)$ and $G(r)$ calculated at the bond critical point are different for a shared interaction or a intermediate interaction. For a shared interaction $V(r)$ is nearly an order higher than $G(r)$. For a intermediate interaction values are of the same order. In our calculations on the carbocations the values of $V(r)$ and $G(r)$ at the 3c−2e bond critical points behave as those from a shared interaction.

Electronic Density in Proponium Cations

J. Phys. Chem. A, Vol. 104, No. 32, 2000 **7589**

TABLE 2: Local Topological Properties in the Bond Critical Points (3,−1) of the Structure 4 (C-Proponium Cation)[a]

bond	R	$\rho(r_c)$	$\nabla^2\rho(r_c)$	λ_1	λ_2	λ_3	$|\lambda_1|/\lambda_3$	e
C_2-C_3	1,495	0,2644	−0,7732	−0,4989	−0,4897	0,2154	2,3161	0,0187
C_1-H	1,079	0,2967	−1,1321	−0,8275	−0,8035	0,4990	1,6583	0,0298
C_2-H	1,081	0,3008	−1,1648	−0,8546	−0,8236	0,5135	1,6643	0,0376
C_3-H_{app}[b]	1,092	0,2803	−1,0057	−0,7259	−0,7188	0,4390	1,6535	0,0100
C_2-H*	1,272	0,1456	−0,1725	−0,2165	−0,1833	0,2273	0,9525	0,1809
C_1-H*	1,188	0,1893	−0,4256	−0,3380	−0,2797	0,1921	1,7595	0,2083

[a] Bond distances are included. Bond distances are expressed in angstroms, and $\rho(r)$ and $\nabla^2\rho(r)$ are expressed in au. [b] H antiperiplanar to the bond C_2-H*.

TABLE 3: Topological Properties of $\nabla^2\rho(r)$ in the VSCC of the Atoms Corresponding to Structure 4[a]

X	R_{X-cp}	$-\nabla^2\rho_{max}$	μ_3	bonded to X
C_3	1.0137	1.1702	−6.40	H
	1.0083	1.2266	−6.64	H
	1.0097	1.2198	−6.62	H
	1.0498	0.8317	−4.19	C_2
C_2	1.7763	0.8317	−4.19	C_3
	0.9720	1.4576	−7.45	H
	0.9763	1.4048	−7.19	H
	0.9477	1.3004	−5.62	H_5
H_5	2.7580	1.3004	−5.62	C_2
C_1	0.9823	1.3814	−7.18	H
	0.9876	1.3116	−6.89	H
	0.9816	1.3812	−7.17	H

[a] Bond charge concentration on X (X = C, H). R_{C-cp} = [au]; $-\nabla^2\rho_{max}$ = [au]; μ_3 = [au].

The structure exhibited by the Laplacian through its collection of valence-shell critical points is summarized for structure **4** in Table 3, where R_{X-cp} corresponds to the radial distance of a bonded charge concentration, μ_3 corresponds to the radial curvature of $-\nabla^2\rho$, the curvature perpendicular to the surface of the sphere of charge concentration. The last column of Table 3 corresponds to the atom bonded to X.

An analysis of the results shows that C_2 and H_5 have the same value of $-\nabla^2\rho$ and μ_3 and that a bonded pair is found between them. No critical points are found between C_1 and H_5 (by scanning the space around C_1 a c.p. was found at 4.34 au, which is too far as to be considered a b.c.p.). This result points out to the evidence of the existence of a 3c−2e bond among $C_2-H_5-C_1$.

In structures **1**, **2** and **3** a c.p., corresponding to a shared interaction, can be characterized between H*−H*. When the three center−two electron bond is formed on the secondary carbon, the H*−H* distance is shorter ($d = 0.867$ Å), and the density of the bond c.p. ($\rho(r_c) = 0.2267$ au) is higher than those formed on a primary H-carbonium ion (structures **1** and **2**, $d = 0.909$ Å and $\rho(r_c) = 0.2198$ and 0.2197 au, respectively). The ellipticity of the H*−H* bond c.p. for structure **1** is the highest ($\epsilon = 1.6274$), indicating that this species is the less stable among the different structures of $C_3H_9^+$ investigated. For the H_2

molecule the values are $\rho(r_c) = 0.2617$ au, $\nabla^2\rho(r_c) = -1.1279$ au and $\epsilon = 0$.

The ellipticities between $C_{(2)}-C_{(1)}$ and $C_{(2)}-C_{(3)}$, as seen in Table 1, are $\epsilon = 0.0112, 0.0274, 0.0236$ and $0.0054, 0.0841, 0.0237$, which are much higher (except only in one case) than the value calculated for the propane molecule ($\epsilon = 0.009$).

Parts a−c of Figure 2 show the contour map of the Laplacian distribution $\nabla^2\rho$ for the H-proponium ions **1**, **2** and **3**, in the plane that contains the carbon atoms (the molecular graph is superimposed). The dotted contour lines correspond to negative values of $\nabla^2\rho$ and display the regions of the space where the electronic density is concentrated. Besides, the full lines indicate the regions where the density is depleted and correspond to positive values of $\nabla^2\rho$. This figure allows one to distinguish the type of bonds, since the critical point at the shared interaction $C_{(1,2)}-H*$ and C_2-H are located in a region of charge accumulation. Figure 2c shows the molecular graph of the 2-H-proponium ion **3** where the c.p. are indicated. The three center two electron bond $C_{(2)}-H*-H*$ is observed. It is interesting to note that there are two critical points in this kind of bond and there is only a c.p. between C_2 and H*. No ring critical points were found.

Table 2 shows the more significant topological local properties at the critical points, c.p. $(3,-1)$ or bond critical points, for structure **4** corresponding to the C-proponium cation, which is the most stable structure among the proponium cations. The bond distances are also reported. The topological distribution of the electronic charge density on the C-proponium cation, **4**, shows significant differences with respect to the structures of the H-proponium cations. The electronic density at the two c.p. of the C−H* bond of the three center bond $C_{(2)}-H*-C_{(1)}$ are rather different. In fact, the density on the bond c.p. of $C_{(1)}-H*$ of the methyl group is higher than the density on the $C_{(2)}-H*$ bond. These results are in agreement with the bond distances calculated for structure **4** (1.188 and 1.272 Å). In the C_1-H* bond the Laplacian of the density is $\nabla^2\rho(r_c) < 0$ and $|\lambda_1|/\lambda_3 > 1$; ($\rho(r_c) = 0.1893$ au and $\nabla^2\rho(r_c) = -0.4256$ au) while in the C_2-H* bond $\nabla^2\rho(r_c) < 0$ (−0.1725 au) but $|\lambda_1|/\lambda_3$ is slightly lower than 1 (0.9525). These results indicate that while the C_1-H* bond corresponds to a shared interaction, the C_2-H* presents a different behavior that seems to be intermediate between a shared and a closed shell interaction. No ring critical point was found for the C-proponium cation.

Figure 2d shows the contour map of the Laplacian distribution $\nabla^2\rho$ for the C-proponium ion **4**, in the plane that contains the carbon atoms (the molecular graph is superimposed). Dotted contour lines correspond to $\nabla^2\rho < 0$ (electronic density concentration) and full lines correspond to $\nabla^2\rho > 0$ (density depletion). This figure allows one to distinguish differences between the C−H bonds involved in the three center−two electron bond. The Figure 2d also shows the molecular graph of the C-proponium ion, **4**, where the c.p. are indicated. It can be observed that the 3c−2e bond presents two critical points though both c.p. are located in a region of charge accumulation.
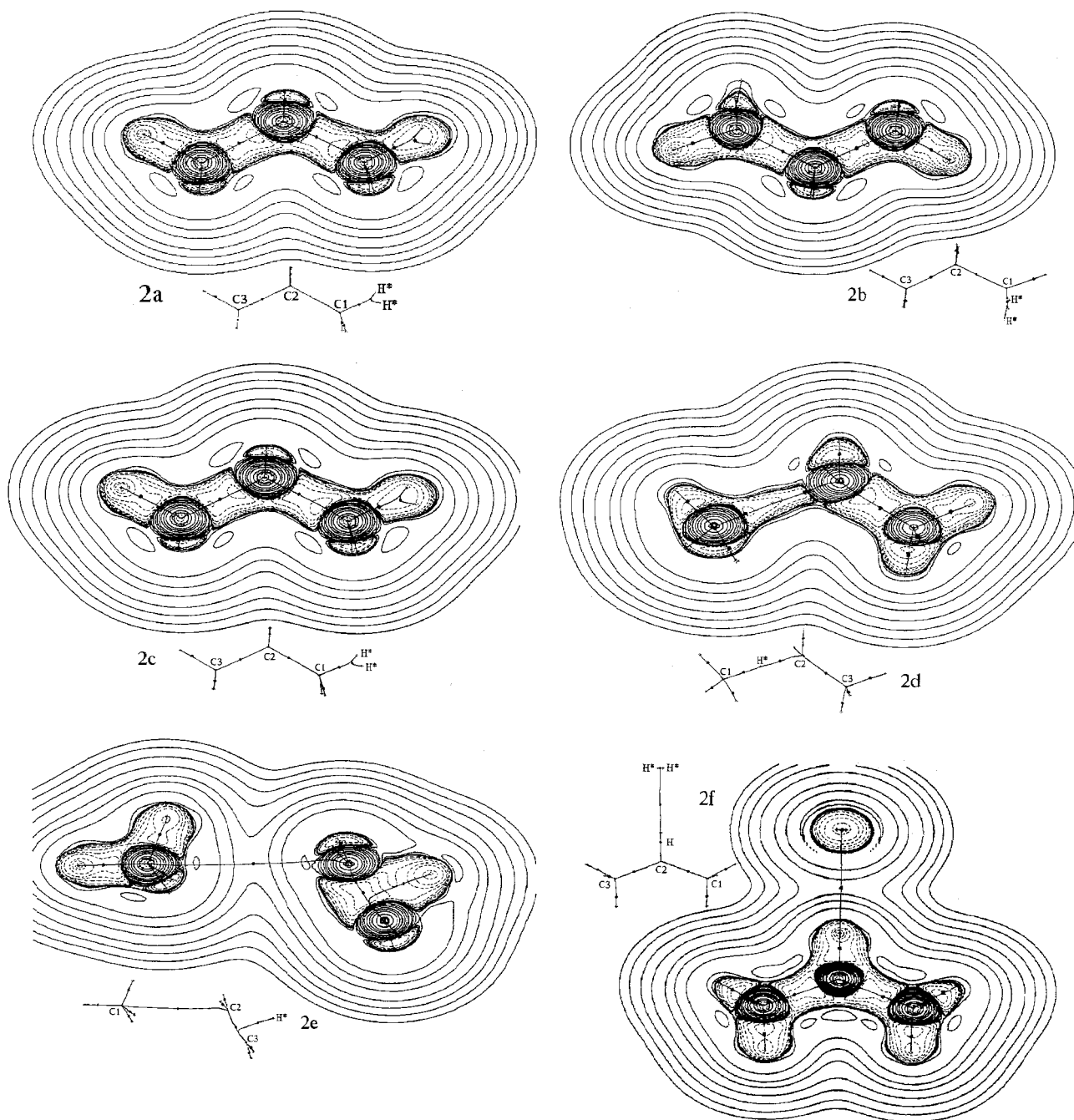
Figure 2. **2a**, **2b**, **2c**, show the contour maps of the Laplacian distribution $\nabla^2\rho$ for the H-proponium ions **1**, **2** and **3**; **2d** shows the contour map of the Laplacian distribution $\nabla^2\rho$ for the C-proponium ion **4**; **2e** and **2f** show the contour maps of the Laplacian distribution $\nabla^2\rho$ for the van der Waals complexes **5** and **6**, in the plane that contains the carbon atoms (the molecular graph are superimposed). The dotted contour lines correspond to negative values of $\nabla^2\rho$ and display the regions of the space where the electronic density is concentrated. In addition, the full lines indicate the regions where the density is depleted and correspond to positive values of $\nabla^2\rho$.

TABLE 4: Local Topological Properties in the Bond Critical Points (3,−1) of the Structure 5^a

bond	R	$\rho(r_c)$	$\nabla^2\rho(r_c)$	λ_1	λ_2	λ_3	$|\lambda_1|/\lambda_3$	ϵ
C_1-C_2	3,133	0,0056	0,0245	−0,0019	−0,0005	0,0269	0,0706	2,5752
C_2-C_3	1,381	0,3222	−1,0030	−0,6805	−0,5479	0,2254	3,0191	0,2420
C_1-H	1,086	0,2795	−0,9991	−0,6936	−0,6865	0,3810	1,8205	0,0105
C_2-H	1,082	0,2991	−1,1768	−0,8658	−0,8470	0,5361	1,6150	0,0221
C_3-H	1,082	0,2973	−1,1593	−0,8512	−0,8364	0,5283	1,6112	0,0176
C_3-H^*	1,280	0,1970	−0,3061	−0,4234	−0,1701	0,2875	1,4727	1,4884

^{a} Bond distances are included. Bond distances are expressed in angstroms, and $\rho(r)$ and $\nabla^2\rho(r)$ are expressed in au.

van der Waals complexes: Table 4 shows the more significant topological local properties at the critical points, c.p. (3,−1) of **5**, corresponding to the interaction between the ethyl cation and the methane molecule. Bond distances are also included. It can be seen that the bond distance C_1-C_2 is 3.133 Å, exhibiting the characteristics of a closed shell interaction,

Electronic Density in Proponium Cations

J. Phys. Chem. A, Vol. 104, No. 32, 2000 **7591**

TABLE 5: Local Topological Properties in the Bond Critical Points (3,−1) of the Structure 6 (MP2 Results in Parentheses)[a]

bond	R	$\rho(r_c)$	$\nabla^2\rho(r_c)$	λ_1	λ_2	λ_3	$|\lambda_1|/\lambda_3$	ϵ
C_2−C_1	1,436	0,2978	−0,9640	−0,5890	−0,5415	0,1665	3,5375	0,0877
		(0,2978)	(−0,9639)	(−0,5888)	(−0,5413)	(0.1661)	(3.5441)	(0,0877)
C_2−C_3	1,436	0,2978	−0,9640	−0,5890	−0,5415	0,1665	3,5375	0,0877
		(0,2978)	(−0,9639)	(−0,5888)	(−0,5413)	(0.1661)	(3.5441)	(0,0877)
C_1−H	1,088	0,2840	−1,0356	−0,7610	−0,7399	0,4653	1,6355	0,0284
		(0,2839)	(−1,0356)	(−0,7609)	(−0,7399)	(0,4653)	(1,6355)	(0,0284)
C_2−H	1,088	0,3029	−1,2091	−0,8948	−0,8593	0,5451	1,6415	0,0413
		(0,3029)	(−1,2090)	(−0,8948)	(−0,8596)	(0,5450)	(1,6417)	(0,0414)
C_3−H	1,088	0,2840	−1,0356	−0,7610	−0,7399	0,4653	1,6355	0,0284
		(0,2839)	(−1,0356)	(−0,7609)	(−0,7399)	(0,4653)	(1,6355)	(0,0285)
C_2−H*	3,561	0,0047	0,0156	−0,0044	−0,0039	0,0239	0,1858	0,1411
		(0,0047)	(−0,0156)	(−0,0044)	(−0,0039)	(0,0239)	(0.1858)	(0,1411)
H*-H*	0,735	0,2664	−1,1238	−0,9077	−0,9064	0,6903	1.3149	0,0014
		(0,2664)	(−1,1382)	(−0,9077)	(−0,9064)	(0,6903)	(1.3148)	(0,0014)

[a] Bond distances are included.

where $\rho(r_c)$ has a low value (0.0056 au) and $\nabla^2\rho > 0$ (0.0245 au). It is interesting to note that the ellipticity of the C_3−H* and C_1−C_2 bonds are high ($\epsilon = 1.4884$ and 2.5752, respectively). As the ellipticity is derived from the relationship between the negative curvatures, its increase is a measure of how far the density distribution is distorted from the axial symmetry of the bond and would explain the higher energy of the complex. Figure 2e shows the contour map of the Laplacian distribution $\nabla^2\rho$ for the van der Waals complex **5**, in the plane that contains the carbon atoms (the molecular graph is superimposed). This figure allows one to see that in the $C_{(3)}$−H* bond the c.p. is localized in a region of charge accumulation, while the c.p. between C_1−C_2 is found in a region of charge depletion, characteristic of closed shell interactions. It is also interesting to note the presence of two critical points in the 3c−2e bond on the $C_2H_5^+$ moiety. In this case the critical points are (or at least one of them) displaced from the line between the nuclei.

Table 5 shows the more significant topological local properties at the critical points c.p. (3,−1) or bond critical points, for structure **6**, corresponding to the interaction between the s-$C_3H_7^+$ cation and the hydrogen molecule. We have also included values (between parenthesis) corresponding to structure **6** calculated from the density matrix obtained at the MP2 level, for comparison purposes. No significant differences were obtained as can be seen in Table 5 where these results are shown.

Taking into account that structure **3** precedes the formation of the van der Waals complex between the isopropyl cation and hydrogen, one can analyze some comparisons between both structures. Table 5 shows the changes in the density charge values of the bonds. In **6** the C−C bonds are shortened and the density on the bond critical points raise, compared with structure **3**. Higher values of ellipticity are also observed in structure **6**. On the other hand, the values of the density charge and the Laplacian for the C_2−H* bond (bond distance 3.561 Å) of structure **6** are diminished compared with respect to the corresponding bonds in structure **3**, showing the characteristics of a closed shell interaction ($\rho(r_c) = 0.0047$ au and $\nabla^2\rho = 0.0156$ au). It can be also shown that the relationship $|\lambda_1|/\lambda_3 < 1$ (0.1841), as it generally happens in a van der Waals interaction. The ellipticity for the C_2−H* bond ($\epsilon = 0.1411$) is grater than in the other C−H bonds ($\epsilon = 0.0413$ for the C_2−H bond), indicating how far the density distribution is from the axial symmetry in this bond ($\lambda_1 \neq \lambda_2$) and may be an indication that this bond could be next to break [20,30].

The corresponding H*−H* bond distance in structure **6** is 0.735 Å, which is shorter than in structure **3** (0.867 Å) and the density charge and Laplacian values are higher, while the

ellipticity value is lower than the corresponding values in structure **3** ($\rho(r_c) = 0.2664$ au and $\nabla^2\rho = -1.1238$ au, $\epsilon = 0.0014$).

Figure 2f shows the contour map of the $\nabla^2\rho$ for the van der Waals complex **6** in the plane that contains the carbon atoms. It can be seen that the C_2−H* bond critical point is localized in a region of charge depletion, characteristic of a closed shell interaction. It can also be seen that the H* atoms of the hydrogen molecule are not located on the plane defined by the carbon atoms, but in a plane almost perpendicular to it, in the direction of the $C_{(2)}$−H bond.

Conclusions

Six different structures were studied: four proponium cations and two van der Waals complexes. Among the proponium cations, the most stable structure corresponds to the C-proponium ion. The topological distribution of the electronic charge density on the C-proponium cation, shows significant differences with respect to structures of the H-proponium cations. The topological properties at the two c.p. of the C−H* bond found in the 3c−2e bond $C_{(2)}$−H*−$C_{(1)}$ are rather different. Both bonds show a shared interaction but the $C_{(2)}$−H* bond due to its value of $|\lambda_1|/\lambda_3 < 1$ (0.9525) can be considered as being between a shared and a closed shell interaction.

The value of $\rho(r_c)$ and $\nabla^2\rho(r_c)$ at the C−H* and H*−H* bond critical points enable to discuss and to predict the nature of the dissociation products. In the secondary H-carbonium, linear structure **3**, ρ is larger for H*−H* than for C−H* (it is the same for the absolute value of $\nabla^2\rho$) therefore one can expect a dissociation into $CH_3CH^+CH_3 + H_2$ corresponding to the structure **6**. In the C-carbonium isomer **4** the values reported in Table 2 for C_1−H* and C_2−H* are consistent with a dissociation into $CH_3CH_2 + CH_4$.

Finally, for the primary H-carbonium isomers (structrures **2** and **3**) the differences between the C−H* and H*−H* values do not clearly indicate a dissociation channel and therefore the transposition yielding structure **4** should to be in compatible with the dissociation into $CH_3CH_2CH_2^+ + H_2$.

Regarding the van der Waals complexes, the most stable one corresponds to the structure that results from the interaction between the isopropyl ion and the hydrogen molecule. It was shown that the interaction between the secondary carbon and the hydrogen molecule corresponds to a closed shell interaction with $\nabla^2\rho > 0$ (0.0156) and $|\lambda_1|/\lambda_3 < 1$ (0.1841).

7592 *J. Phys. Chem. A, Vol. 104, No. 32, 2000*

Okulik et al.

References and Notes

(1) Olah, G. A.; Schlosberg, R. H. *J. Am. Chem. Soc.* **1968**, *90*, 2726.

(2) Olah, G. A.; Klopman, G.; Schlosberg, R. H. *J. Am. Chem. Soc.* **1969**, *91*, 3261.

(3) Hogeveen, H.; Bickel, A. F. *Recl. Trav. Chim. Pays-Bas.* **1969**, *88*, 371.

(4) Olah, G. A. *Angew. Chem., Int. Ed. Engl.* **1973**, *12*, 171.

(5) Olah, G. A. *Carbocations and Electrophilic Reaction*; Wiley: New York, 1973.

(6) Haag, W. O.; Dessau, R. M. *Proceedings of the 8th International Congress in Catalysis*; Verlag Chemie and Dechema: Weinheim and Berlin, 1984; pp 305−316.

(7) Gianetto, G.; Sanrase, S.; Guisnet, M. *J. Chem. Soc., Chem. Commun.* **1986**, 1302.

(8) Mota, C. J. A.; Martins, *J. Chem. Soc., Chem. Commun.* **1991**, 171.

(9) Mota, C. J. A.; R. L. Nogueira, L.; Kover, W. B. *J. Am. Chem. Soc.* **1992**, *114*, 1121.

(10) Dyczmons, V.; Staemmler, V.; Kutzelnigg, W. *Chem. Phys. Lett.* **1970**, *5*, 361.

(11) Raghavachari, K.; Whiteside, R. A.; Pople, J. A. Schleyer, P. V. R. *J. Am. Chem. Soc.* **1981**, *103*, 5649.

(12) Schleyer, P. v. R.; Carneiro, J. W. M. *J. Comput. Chem.* **1992**, *13*, 997.

(13) Kim, S. A.; Schreiner, P. R.; Schleyer, P. v. R.; Schafer, H. F., III *J. Phys. Chem.* **1993**, *97*, 12232.

(14) Schreiner, P. R.; Kim, S. J.; Schafer, H. F., III; Schleyer, P. v. R. *J. Chem. Phys.* **1993**, *99*, 3716.

(15) Scuseria, G. E. *Nature* **1993**, *366*, 512.

(16) Kolbuszewski, M.; Bunker, P. R. *J. Chem. Phys.* **1996**, *105*, 3649.

(17) Muller, H.; Kutzelnigg, W.; Noga, J.; Klopper, W. J. *J. Chem. Phys.* **1997**, *106*, 1863.

(18) Olah, G. A.; Rasul, G. *Acc. Chem. Res.* **1997**, *30*, 245.

(19) Bischof, P. K.; Dewar, M. J. S. *J. Am. Chem. Soc.* **1975**, *97*, 2278.

(20) Kohler, H. J.; Lischka, H. *Chem. Phys. Lett.* **1978**, *58*, 175.

(21) Poirier, R. A.; Constantin, E.; Abbé, J. C.; Peterson, M. R.; Csizmadia, I. G. *J. Mol. Struct.* (*THEOCHEM*) **1982**, *88*, 343.

(22) Hirao, K.; Yamabe, S. *Chem. Phys.* **1984**, *89*, 237.

(23) Carneiro, J. W. M.; Schleyer, P. v. R.; Saunders, M.; Remington, R.; Schaefer, H. F. III; Rauk, A.; Sorensen, T. S. *J. Am. Chem. Soc.* **1994**, *116*, 3483.

(24) Bader, R. F. W.; Anderson, S. G.; Dake, A. J. *J. Am. Chem. Soc.* **1979**, *101*, 1389.

(25) Bader, R. F. W.; Nguyen-Dang, T. T.; Tal, Y. *J. Chem. Phys.* **1979**, *70*, 6316.

(26) Bader, R. F. W. *J. Chem. Phys.* **1980**, *73*, 2871.

(27) Bader, R. F. W.; Nguyen-Dang, T. T. *Adv. Quantum Chem.* **1981**, *14*, 6310.

(28) Mulliken, R. S. *J. Chem. Phys.* **1955**, *23*, 1833.

(29) Bader, R. F. W.; Slee, T. S.; Cremer, D.; Kraka, E. *J. Am. Chem. Soc.* **1983**, *105*, 5061.

(30) Cremer, D.; Kraka, E.; Slee, T. S.; Bader, R. F. W.; Lau, C. D. H.; Nguyen-Dang, T. T.; MacDougall, P. J. *J. Am. Chem. Soc.* **1983**, *105*, 5069.

(31) Okulik, N.; Peruchena, N. M.; Esteves, P. M.; Mota, C. J. A.; Jubert, A. *J. Phys. Chem. A* **1999**, *103*, 8491.

(32) Esteves, P. M.; Mota, C. J. A.; Ramirez-Solis, A.; Hernández-Lamoneda, R. *J. Am. Chem. Soc.* **1998**, *120*, 3213.

(33) M. J. Frisch, G. W. Trucks, H. B. Schlegel, P. M. W. Gill, B. G. Johnson, M. A. Robb, J. R. Cheeseman, T. Keith, G. A. Petersson, J. A. Montgomery, K. Raghavachari, M. A. Al-Laham, V. G. Zakrzewski, J. V. Ortiz, J. B. Foresman, J. Cioslowski, B. B. Stefanov, A. Nanayakkara, M. Challacombe, C. Y. Peng, P. Y. Ayala, W. Chen, M. W. Wong, J. L. Andres, E. S. Replogle, R. Gomperts, R. L. Martin, D. J. Fox, J. S. Binkley, D. J. DeFrees, J. Baker, J. P. Stewart, M. Head-Gordon, C. Gonzalez, J. A. Pople. *Gaussian 94*, Revision D. 3; Gaussian, Inc.: Pittsburgh, PA, 1995.

(34) Schmidt, M. W.; Baldridge, K. K.; Boatz, J. A.; Elbert, S. T.; Gordon, M. S.; Jensen, J. H.; Koseki, S.; Matsunaga, N.; Nguyen, K. A.; Su, S. J. Windus, T. L.; Dupuis, M.; Montgomery, J. A. *J. Comput. Chem.* **1993**, *14*, 1347.

(35) Klieger-Konig, W.; Bader, R. F. W.; Tag, T. H. *J. Comput. Chem.* **1982**, *3*, 317.

(36) Bader, R. F. W. *J. Chem. Phys.* **1980**, *73*, 2871.

(37) Bader, R. F. W. *Atoms in Molecules. A Quantum Theory*; Claredon Press: Oxford, 1990.

(38) Gillespie, R. J. *Molecular Geometry*; Van Nostrand Reinhold: London, 1972.